Cancer cell-derived long pentraxin 3 (PTX3) promotes melanoma migration through a toll-like receptor 4 (TLR4)/NF-κB signaling pathway

M. Rathore, Christophe Girard, M. Ohanna, M. Tichet, R. Ben Jouira, E. Garcia, F. Larbret, M. Gesson, S. Audebert, J.-P. Lacour, et al.

Oncogene
https://doi.org/10.1038/s41388-019-0848-9

ARTICLE

Cancer cell-derived long pentraxin 3 (PTX3) promotes melanoma migration through a toll-like receptor 4 (TLR4)/NF-κB signaling pathway

M. Rathore[1,2,3] · C. Girard[1,2] · M. Ohanna[1,2] · M. Tichet[1,6] · R. Ben Jouira[1] · E. Garcia[1] · F. Larbret[1,2] · M. Gesson[1] · S. Audebert[4] · J.-P. Lacour[5] · H. Montaudié[5] · V. Prod'Homme[1,2] · S. Tartare-Deckert[1,2] · M. Deckert[1,2]

Received: 25 May 2018 / Revised: 30 March 2019 / Accepted: 28 April 2019

Abstract

Cutaneous melanoma is one of the most aggressive cancers characterized by a high plasticity, a propensity for metastasis, and drug resistance. Melanomas are composed of phenotypically diverse subpopulations of tumor cells with heterogeneous molecular profiles that reflect intrinsic invasive abilities. In an attempt to identify novel factors of the melanoma invasive cell state, we previously investigated the nature of the invasive secretome by using a comparative proteomic approach. Here, we have extended this analysis to show that PTX3, an acute phase inflammatory glycoprotein, is one such factor secreted by invasive melanoma to promote tumor cell invasiveness. Elevated PTX3 production was observed in the population of $MITF^{low}$ invasive cells but not in the population of $MITF^{high}$ differentiated melanoma cells. Consistently, MITF knockdown increased PTX3 expression in $MITF^{high}$ proliferative and poorly invasive cells. High levels of PTX3 were found in tissues and blood of metastatic melanoma patients, and in BRAF inhibitor-resistant melanoma cells displaying a mesenchymal invasive $MITF^{low}$ phenotype. Genetic silencing of PTX3 in invasive melanoma cells dramatically impaired migration and invasion in vitro and in experimental lung extravasation assay in xenografted mice. In contrast, addition of melanoma-derived or recombinant PTX3, or expression of PTX3 enhanced motility of low migratory cells. Mechanistically, autocrine production of PTX3 by melanoma cells triggered an IKK/NFκB signaling pathway that promotes migration, invasion, and expression of the EMT factor TWIST1. Finally, we found that TLR4 and MYD88 knockdown inhibited PTX3-induced melanoma cell migration, suggesting that PTX3 functions through a TLR4-dependent pathway. Our work reveals that tumor-derived PTX3 contributes to melanoma cell invasion via targetable inflammation-related pathways. In addition to providing new insights into the biology of melanoma invasive behavior, this study underscores the notion that secreted PTX3 represents a potential biomarker and therapeutic target in a subpopulation of $MITF^{low}$ invasive and/or refractory melanoma.

Introduction

Melanoma is the leading cause of skin cancer-related deaths, whose incidence has increased dramatically in the past 30 years. Melanoma arises from neural-crest-derived melanocytes found in the basal layer of the epidermis and responsible for melanin production and pigmentation. Early metastatic spread, intratumor heterogeneity, and therapeutic

These authors contributed equally: M. Deckert, S. Tartare-Deckert

Supplementary information The online version of this article (https://doi.org/10.1038/s41388-019-0848-9) contains supplementary material, which is available to authorized users.

✉ S. Tartare-Deckert
tartare@unice.fr

✉ M. Deckert
deckert@unice.fr

[1] Université Côte d'Azur, INSERM, C3M, Nice, France

[2] Equipe labellisée Ligue Contre le Cancer 2016, Nice, France

[3] The Hormel Institute, University of Minnesota, Austin, MN, USA

[4] Aix-Marseille University, CNRS, INSERM, Institut Paoli-Calmettes, CRCM, Marseille, France

[5] Université Côte d'Azur, CHU Nice, Nice, France

[6] Present address: Laboratory of Translational Oncology, ISREC, EPFL, Lausanne, Switzerland

Published online: 28 June 2019

resistance are hallmarks of melanoma. During the last years, much has been learned about the genetic and epigenetic driver events of tumor initiation, progression, and response to targeted therapies. Activating mutations of the *BRAF* proto-oncogene, which are the most prevalent mutations predict clinical efficacy to BRAF inhibitors such as vemurafenib in BRAF-mutated metastatic melanomas; and *NRAS* mutant tumors are known to exhibit sensitivity to MEK inhibition [1, 2]. Despite recent breakthroughs in melanoma treatments with the combination of targeted therapies using BRAF and MEK inhibitors and immunotherapies using checkpoint-blocking antibodies, resistance invariably develops and the prognosis remains dismal for most patients. Notably, current targeted therapies have even been shown to promote a mesenchymal-like invasive cell state and metastasis of resistant melanoma cells [3].

The acquisition of an invasive behavior is one of the key events in the progression to aggressive and deadly melanoma. Thus, identification of tumor cell intrinsic and extrinsic factors and characterization of the molecular mechanisms that drive this behavior are essential to our understanding of how melanoma metastasis develops, and to the development of novel therapeutic strategies. Emerging evidence support that progression to metastasis involves a series of reversible phenotypic changes in tumor cells. Under microenvironmental influences melanoma cells can undergo transcriptional reprogramming and switch between two different dominant states, either proliferative and poorly invasive or invasive and poorly proliferative, both being characterized by distinct gene expression signatures [3–6]. Levels and activity of microphthalmia-associated transcription factor (MITF), the melanocyte lineage-restricted transcription factor, are key determinants of the melanoma phenotype switch and tumor cell plasticity. The "proliferative" cellular state expresses higher levels of MITF than the "invasive" state. Importantly, the MITF^{low} invasive signature has been associated with intrinsic resistance to new drugs targeting mutant BRAF and MEK [3, 7, 8]. Finally, acquisition of migratory and invasive traits by melanoma cells also involved modulation of epithelial–mesenchymal transition (EMT)-inducing transcription factors expression, including members of the SNAIL, TWIST, and ZEB families [9–11].

Tumor cell-secreted factors play a key role in the process of malignant progression via their ability to regulate cell autonomous signaling and paracrine stroma communication. Drivers of melanoma invasion include such autocrine signals propagated by secreted factors that may thus represent potential candidate molecules for diagnosis and specific anti-invasive therapies. By proteomic profiling of metastatic and non-metastatic melanomas we recently identified a spectrum of secreted factors and inflammatory mediators that were enriched in conditioned medium (CM) of metastatic cells compared to non-metastatic cells [12]. Of potential interest, the long pentraxin 3 (PTX3) was found abundantly produced by metastatic melanoma cells. PTX3 is an evolutionarily conserved pattern recognition molecule involved in innate immune response, complement activation and inflammation, and have been linked to diseases such as cancer [13, 14]. A complex role of PTX3 in cancer, either as an oncosuppressor or a protumorigenic factor, is emerging [15, 16]. The goal of this study was to analyze the autocrine function of PTX3 in melanoma cell invasive signaling and metastasis and to determine the relevance of these observations to human disease. We show that PTX3 is a key factor secreted by a MITF^{low} invasive subpopulation of melanoma, and contributes to tumor cell migration and invasion in vitro and in vivo. Importantly, tissues and systemic PTX3 levels are elevated in a fraction of metastatic melanoma patients, and in mesenchymal drug-resistant melanoma cells. Mechanistically, we found that PTX3 functions through a TLR4/MYD88/IKK/NF-κB feed-forward signaling pathway to mediate the expression of EMT transcription factor TWIST1, and to promote melanoma migration. In summary, our results point to PTX3 as a potentially useful biomarker for advanced melanoma and as an anti-melanoma therapeutic target.

Results

PTX3 expression is associated with an invasive melanoma cell state

Using quantitative mass spectrometry analysis [12], the pentraxin-related protein PTX3 was found enriched in CM from metastatic 1205Lu cells compared to the poorly invasive 501Mel cells (Supplementary Table 1). Antibody arrays analysis confirmed that PTX3 is abundantly produced by metastatic melanoma cells in addition to other proteins involved in migration and inflammation (IL-1α, IL-6, IL-8, MCP-1, TNFsR1, CCL2), matrix remodeling and adhesion (TSP1, TIMP1) (Supplementary Fig. 1). Direct dosage by enzyme-linked immunosorbent assay (ELISA) and immunoblot analysis of PTX3 in CM obtained from different malignant melanoma cells showed that PTX3 was preferentially produced by 1205Lu and A375 cell lines (Fig. 1a, b). PTX3 was also secreted by cultures of primary tumor cells from metastatic melanoma patients (Pt1 and Pt2) (Fig. 1a). It is recognized that melanoma cells can switch from a proliferative and poorly invasive MITF^{high} phenotype to an invasive and poorly proliferative MITF^{low} phenotype [4]. Given our observations, we thus searched publicly available gene expression data sets for PTX3 expression in proliferative vs. invasive melanoma cell population within the Mannheim, Philadelphia, and Zurich cohorts (GSE4843,

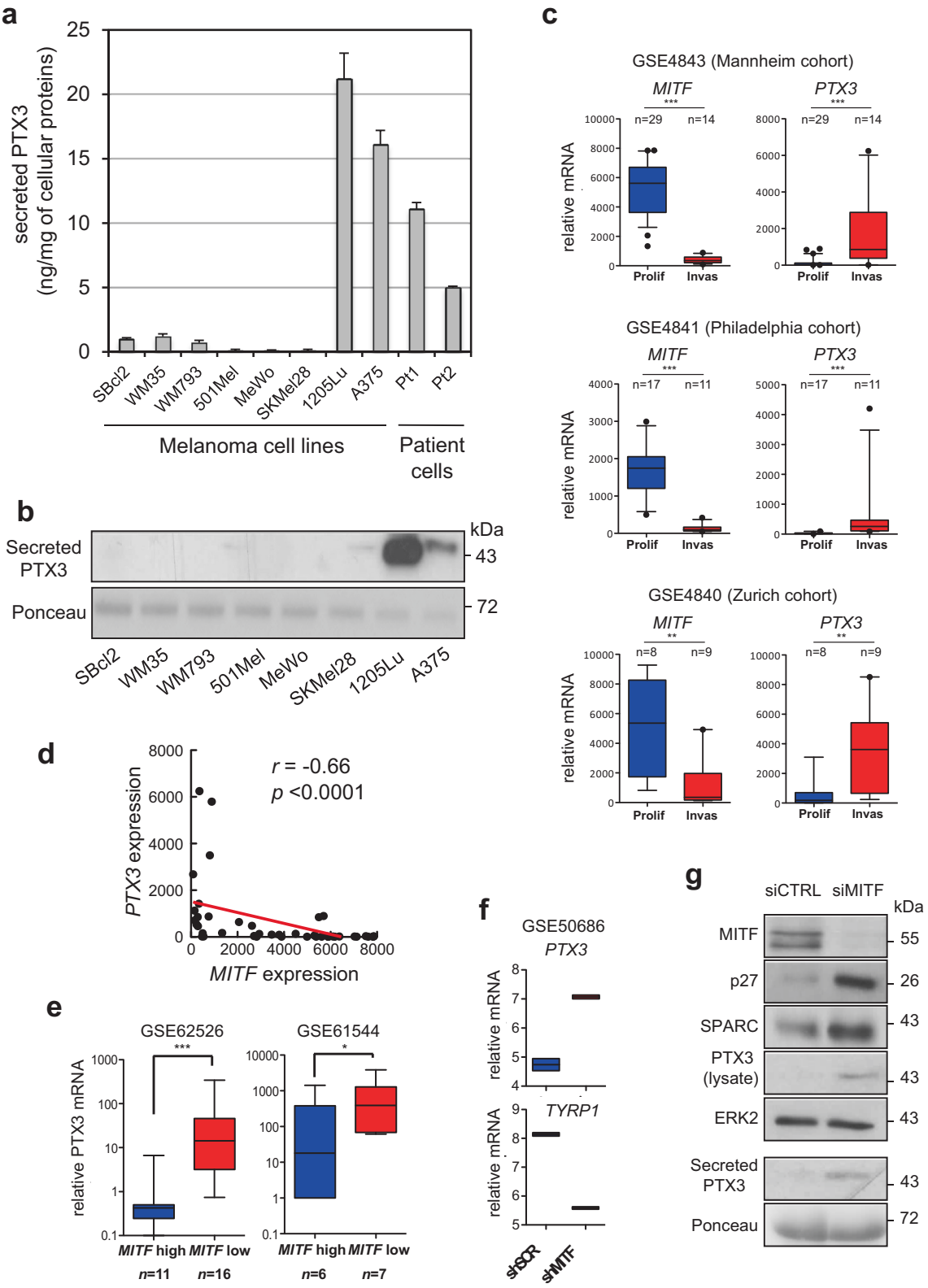

GSE4841, and GSE4840 data sets, respectively) and found an inverse correlation between *PTX3* and *MITF* expression across proliferative and invasive cell states (Fig. 1c, d). Furthermore, values extracted from additional GEO databases revealed that *PTX3* expression increased in MITF^{low} cells compared to MITF^{high} cells (GSE62526 and

◀ **Fig. 1** PTX3 expression is associated with an invasive MITF^{low} melanoma cell state. **a** ELISA analyses of PTX3 secretion in CM of different melanoma cell lines and patient short-term cultures. Equal amounts of CM from SBcl2, WM35, WM793, 501Mel, MeWo, SKMel28, 1205Lu, A375, and melanoma patient cells (Pt1, Pt2) were subjected to PTX3 ELISA. Data represent the mean concentration of PTX3 in CM ± s.e.m of duplicate determinations. **b** Equal amounts of CM from melanoma cell lines were immunoblotted with PTX3 antibody. Ponceau staining was used as a loading control for secreted proteins. **c** Box and whisker plots (10th to 90th percentile) show *MITF* and *PTX3* expression across proliferative vs. invasive cell states of melanoma cultures within the Mannheim, Philadelphia, and Zurich cohorts (GSE4843, GSE4841, and GSE4840 data sets). *P*-values were calculated by unpaired two-tailed Mann–Whitney test. **d** Spearman's correlation analysis of the MITF and PTX3 mRNA expression across the Mannheim melanoma cohort (GSE4843). **e** *PTX3* mRNA expression in melanoma cell lines classified based on high (*MITF* high) or low (*MITF* low) levels of *MITF* expression. Box and whisker plots (10th to 90th percentile) show normalized *PTX3* expression values mined from publicly available data sets (GSE62526 and GSE61544). *P*-values were calculated by unpaired two-tailed Mann–Whitney test. **f** *PTX3* and *TYRP1* gene mRNA in melanoma cells depleted (shMITF) or not (shSCR) of MITF. Box plots depict *PTX3* expression values extracted from a GEO data set (GSE50686). **g** 501Mel cells were transfected with siCTRL or siMITF for 3 days. Total cell lysates and CM were analyzed by immunoblotting with antibodies against MITF, p27Kip1, SPARC, PTX3, and ERK2 as a loading control. Ponceau staining was used as a loading control for secreted proteins. ***$P < 0.0001$; **$P < 0.01$; *$P < 0.05$

GSE61544) (Fig. 1e) and that short-hairpin RNA (shRNA)-mediated depletion of MITF in COLO829 melanoma cells upregulated PTX3 mRNA expression (GSE50686) (Fig. 1f). Finally, knockdown of MITF expression in the poorly invasive cell line 501Mel was associated with increased levels and secretion of PTX3 (Fig. 1g). Consistent with our previous report [5], the expression of the mesenchymal marker SPARC and p27^{Kip1} was also augmented following MITF depletion in 501Mel cells. Altogether our data identify high levels of PTX3 in MITF^{low} invasive melanoma cells.

PTX3 is upregulated during human metastatic melanoma disease and acquisition of mesenchymal drug resistance

The finding that PTX3 level was associated with a melanoma invasive signature prompted us to examine its expression in metastases and blood samples from melanoma patients. In silico data analysis of PTX3 expression in public databases showed that PTX3 mRNA was increased in metastatic melanoma compared to benign skin lesions (nevi) (Fig. 2a). In addition, the examination of *PTX3* in melanoma patients from The Cancer Genome Atlas (TCGA) data sets revealed that *PTX3* alterations (*PTX3* amplifications and mRNA upregulation) were associated with a trend toward shorter disease-free progression ($P = 0.0151$) and shorter overall survival ($P = 9.872e\text{-}3$) (Fig. 2b). Interestingly, gene set enrichment analysis (GSEA) showed that high PTX3 levels in melanoma tumors positively correlated with Epithelial-to-Mesenchymal Transition (EMT) and Inflammatory Response gene signatures (Fig. 2c).

Immunohistochemical analysis of PTX3 in melanoma tissue microarrays showed that a marked PTX3 cytoplasmic and membranous immunoreactivity in malignant melanoma at stage IV (3 out of 10) compared to four adjacent normal skin tissues. In contrast, malignant melanoma at stage III (6 out of 6) showed low to medium levels of PTX3 (Fig. 2d, e and Supplementary Fig. 2). Consistently, the amount of circulating PTX3 in blood from patients with stage IV metastatic disease ($n = 16$) was significantly increased in diseased (7.98 ± 5.12 ng/ml) compared to healthy subjects ($n = 10$) (2.36 ± 1.15 ng/ml) samples (Fig. 2f). These observations indicate that high PTX3 levels correlated with melanoma cells from advanced metastatic disease.

Recent findings indicate that by switching from a proliferative MITF^{high}/AXL^{low} to a mesenchymal invasive MITF^{low}/AXL^{high} state, melanoma cells can acquire resistance to targeted therapies [3, 7]. We thus investigated the potential link between PTX3 expression and acquired resistance to BRAF inhibitors. Immunoblot analyses performed on isogenic pairs of sensitive and vemurafenib-resistant melanoma cells [17] revealed that MITF^{low}-resistant cells M229R and M238R expressed and secreted high levels of PTX3 when compared to MITF^{high} drug-sensitive parental cells M229P and M238P (Fig. 3a, b). As expected, the mesenchymal markers Fibronectin and PDGFR-β were also upregulated in the two resistant cell lines (Fig. 3a) [18]. Importantly, our observations were clinically supported in public gene expression data sets showing that *PTX3* increased in progressing tumors biopsies during therapy with BRAFi (vemurafenib or dabrafenib) or MEKi (trametinib) (Fig. 3c). Our analysis of the CM prepared from melanoma cells derived from a relapsing melanoma patient further showed that PTX3 and Fibronectin production by melanoma cells increased following the acquisition of mesenchymal resistance to vemurafenib (Fig. 3d). Altogether, our findings hence link PTX3 expression to a subpopulation of inflammatory, dedifferentiated and invasive melanoma cells, which could be associated with poor prognosis.

Melanoma-derived PTX3 promotes tumor cell migration

We next investigated the contribution of PTX3 to melanoma cell migration. To this end, the migratory ability of PTX3-depleted cells was tested in Boyden chamber assays. Knockdown of PTX3 in 1205Lu and A375 cells using two different non-overlapping PTX3-targeting small-interfering

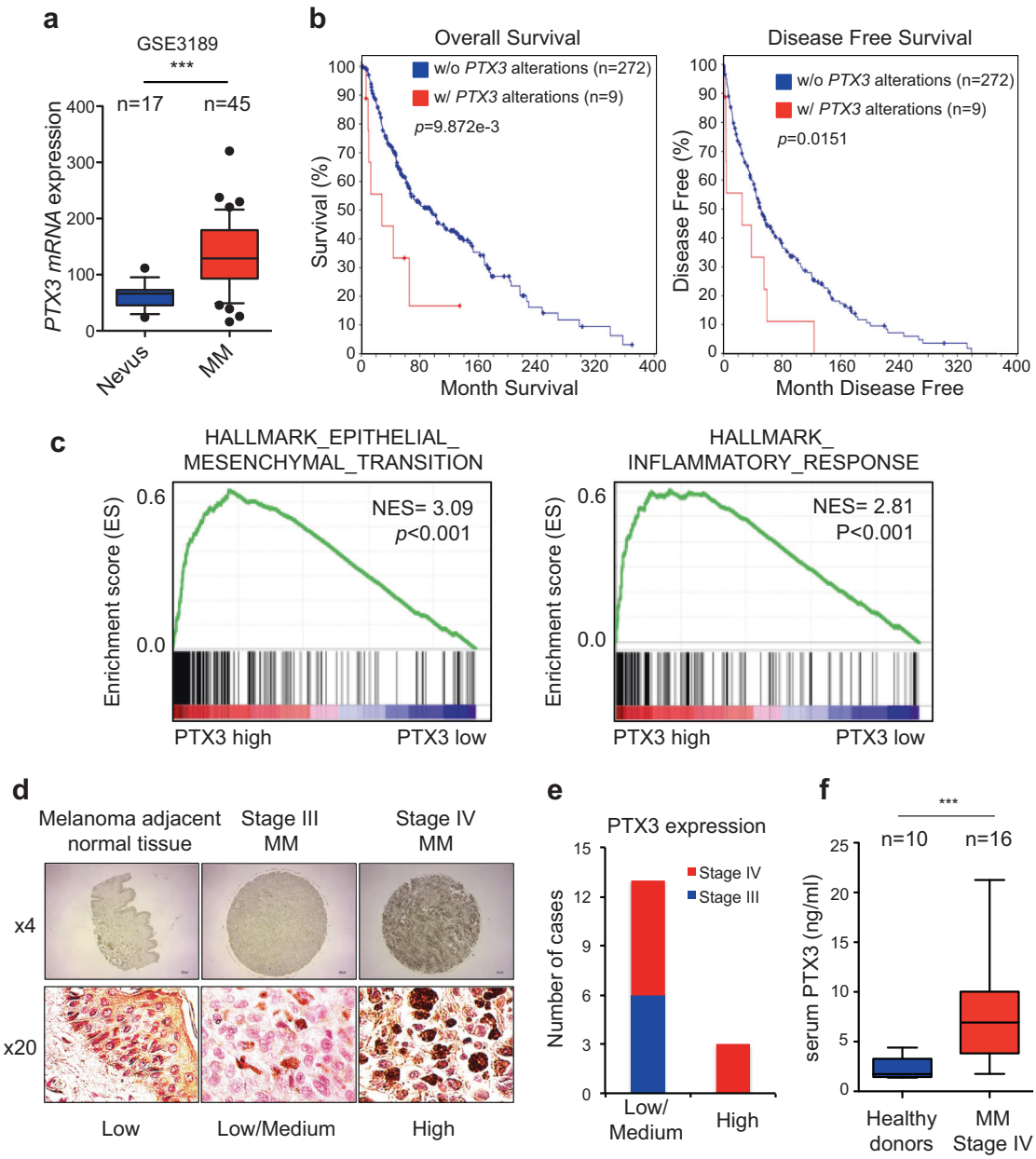

Fig. 2 Expression of PTX3 in malignant melanoma. **a** Box and Whisker plots (10th to 90th percentile) show PTX3 mRNA expression in metastatic vs. benign skin lesions (nevi) (GSE3189). *P*-values were calculated by unpaired two-tailed Mann–Whitney test. **b** Kaplan–Meier overall survival and disease-free survival curves for melanoma patients with or without *PTX3* alterations (*PTX3* amplifications and mRNA upregulation). Data were retrieved from the skin melanoma TCGA database using cBioPortal (cbioportal.org). Data were restricted to AMP EXP ≥ 2 to exclude patients with *PTX3* deletion. Median months survival: 28 vs. 94.9 ($P = 9.872e\text{-}3$, logrank test). Median months Disease-free: 25.5 vs. 51.4 ($P = 0.0151$, logrank test). **c** Gene set enrichment analysis (GSEA) of genes that positively (red) or negatively (blue) correlate with PTX3 expression in skin melanoma TCGA database. Data represent plots for the top two gene sets most significantly enriched. **d** Immunohistochemical analysis of PTX3 levels on human melanoma tissue microarrays. Data show representative IHC images of PTX3 expression in melanoma adjacent normal skin tissues, stage III malignant melanoma and stage IV malignant melanoma according to the tumor-node-metastasis (TNM) classification system. PTX3 was counterstained with hematoxylin. Top panels, representative images of the melanoma tissue microarray cores. Bottom panels, representative images of the microarray at high magnification. Samples were scored as low, medium or high PTX3 expression. **e** Quantification of PTX3 expression in stage III (six cases) and stage IV (ten cases) melanoma tissue arrays from **d** and Supplementary Fig. 2. **f** Serum analysis for PTX3 from metastatic melanoma (MM) patients ($n = 16$) compared to healthy donors ($n = 10$). Error bars represent mean ± s.e.m. $^{***}P < 0.0005$, unpaired two-tailed Mann–Whitney's test

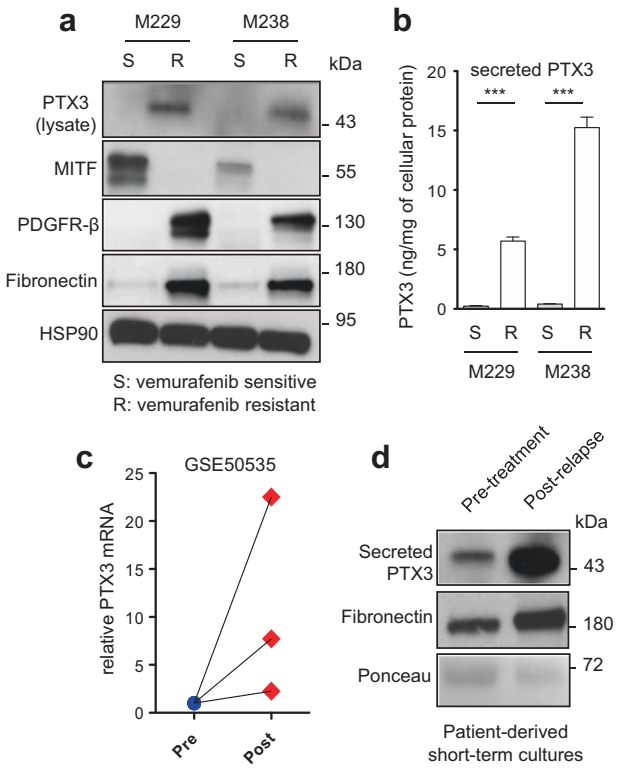

Fig. 3 Increased PTX3 expression in BRAF inhibitor mesenchymal resistant melanoma. **a** Immunoblot analyses of PTX3 expression in isogenic pairs of sensitive (M229S, M238S) and vemurafenib-resistant melanoma cells (M229R, M238R). Total cell lysates were immunoblotted with antibodies against PTX3, MITF, PDGFR- β, Fibronectin, and HSP90 as a loading control. **b** ELISA analyses of PTX3 secretion in CM derived from the above sensitive and resistant melanoma cells. PTX3 levels in CM were normalized against the amount of cellular proteins in each condition. Data represent the mean concentration of PTX3 in CM ± s.e.m of duplicate determinations. $^{**}P < 0.01$; $^{***}P < 0.001$ as determined by two-way ANOVA and Bonferroni post-tests. **c** P*TX3* gene expression levels in data sets (GSE5053) derived from three-paired tumor biopsies of melanoma patients before (Pre) and after (Post) development of resistance to BRAF inhibitors. **d** CM was prepared from melanoma cell cultures derived from one patient before (Pre) and after (Post) development of drug resistance and immunoblotted with PTX3 and Fibronectin antibodies. Ponceau staining was used as a loading control for secreted proteins

RNAs (siRNAs; siPTX3#1 and siPTX3#2) inhibited the chemotactic migration of melanoma cells towards serum compared to cells transfected with a non-targeting siRNA (siCTRL) (Fig. 4a). Importantly, PTX3 knockdown, which abrogated PTX3 secretion, had no significant effect on cell viability (Supplementary Fig. 3c). Depleting PTX3 also blocked the migration of invasive M229R and M238R BRAFi-resistant cell lines and of metastatic melanoma cells derived from a patient (Pt1) (Fig. 4a). Conversely, the stable expression of PTX3 in PTX3-negative cells 501Mel and SKMel28 increased cell migration (Fig. 4b) (Supplementary Fig. 4). Addition of exogenous recombinant PTX3 rescued the migratory ability of PTX3-depleted A375 and 1205Lu cells (Fig. 4c and Supplementary Fig. 5), suggesting that PTX3 promotes melanoma cell migration in an autocrine manner following its secretion by the cancer cell. To test this hypothesis, we carried out in vitro scratch assays using the non-invasive PTX3-negative 501Mel cells incubated with CM produced by invasive PTX3-positive 1205Lu cells. As shown in Fig. 4d, the addition of CM produced by 1205Lu cells transfected by non-targeting siRNA enhanced the migration of 501Mel cells in the wound gap, whereas adding CM produced by PTX3-depleted 1205Lu cells had no significant effect on 501Mel cell migration. Using 1205Lu CMs that were immuno-depleted of PTX3, we confirmed that secreted PTX3 is required to induce melanoma cell migration (Fig. 4e). Of note, PTX3-expressing 501Mel cells displayed increased cell motility in scratch assays when compared to control PTX3-negative 501Mel cells (Supplementary Fig. 6). In addition, we found that recombinant PTX3 enhanced the migration of another non-invasive PTX3-negative melanoma cell line, SKMel28 (Fig. 4f), indicating that melanoma-derived PTX3 has a direct effect on tumor cell motility.

PTX3 expression increases melanoma invasiveness and lung extravasation

Our observations led us to investigate whether PTX3 participates to melanoma cell invasion. Matrigel invasion assays revealed that siRNA-mediated depletion of PTX3 reduced the invasive migration of 1205Lu, A375, and M229R (Fig. 5a). Interestingly, exogenous recombinant PTX3 restored the impaired invasiveness of PTX3-depleted 1205Lu cells (Fig. 5b). Conversely, stable expression of PTX3 in PTX3-negative SKMel28 cells increased the capacity of melanoma cells to invade matrigel (Fig. 5c). To investigate further the activity of PTX3 in melanoma invasion, A375 and WM266.4 cell spheroids were implanted into gels of type I collagen and three-dimensional (3D) tumor cell invasion was evaluated by microscopy. Whereas knockdown of PTX3 had no significant effect on spheroid growth rate, the depletion of PTX3 impaired melanoma invasion into collagen of both cell lines (Fig. 5d, Supplementary Fig. 7). Consistently, zymographic analysis of the invasion-related matrix metalloproteinase MMP-9 revealed a decrease of its collagenase activity in PTX3-depleted melanoma cells compared to control (Fig. 5d). Tumor cell extravasation is a required early step during tissue colonization and metastatic spread [19]. To examine how PTX3 participates to this process, we assessed the effect of PTX3 knockdown in transendothelial migration of 1205Lu cells on monolayers of TNFα-activated HUVECs. Compared to control siRNA-transfected cells, the transmigration of PTX3-silenced melanoma cells was markedly reduced (Fig. 5e). Importantly, the reduced potential of

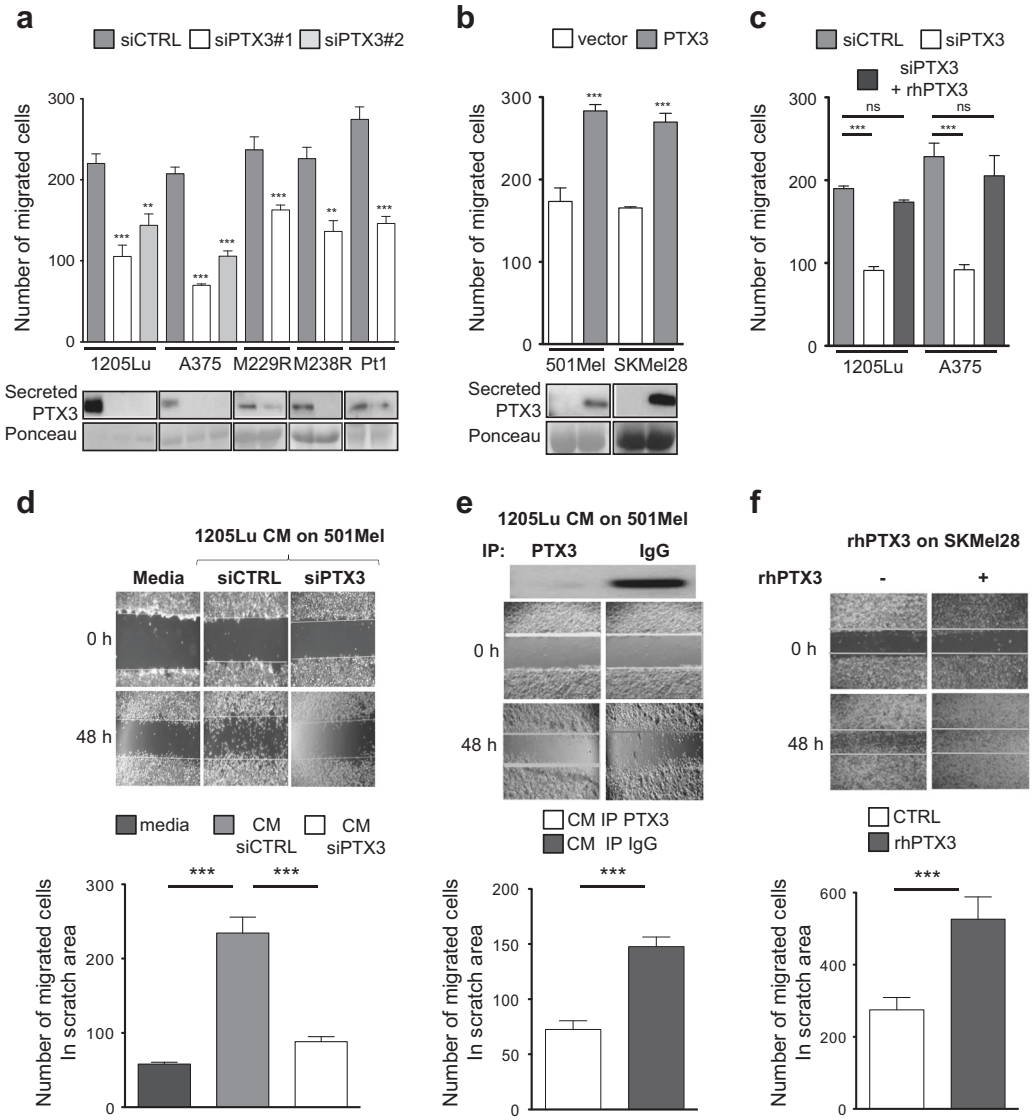

Fig. 4 Melanoma-derived PTX3 promotes tumor cell migration. **a** A375, 1205Lu, M229R, M238R, and patient-derived (Pt1) melanoma cells were transfected with siCTRL or two different siPTX3. After 3 days, serum-stimulated migration assays were performed for 4 h using Transwell inserts. Bar graphs show mean number of migrated cells ± s.e.m ($n = 3$ independent experiments). Lower panel: CMs from transfected cells were immunoblotted with anti-PTX3. **b** Transwell migration assays for melanoma cells (501Mel, SKMel28) stably expressing PTX3 were performed for 16 h. Bar graphs show mean ± s.e.m ($n = 3$ independent experiments). PTX3 immunoblots are shown in lower panel. **c** A375 and 1205Lu cells were transfected with siCTRL or siPTX3. After 3 days, Transwell migration assays were performed in the presence or not of rhPTX3 (100 ng/ml). Bar graphs represent mean ± s.e.m ($n = 3$ independent experiments). **d** Confluent 501Mel cells were scratched and CMs from 1205Lu depleted or not for PTX3 were added. Cells were photographed under a phase contrast microscope after 48 h (upper panels) and migrating cells in scratch area were quantified (lower panels). Bar graphs represent means ± s.e.m. ($n = 3$ independent experiments). **e** Motility of 501Mel cells was assayed by scratch assays in the presence or not of 1205Lu CMs cleared from PTX3 by immunoprecipitation (IP). Upper panel: PTX3 immunoblot of the cleared CMs. Bar graphs show mean ± s.e.m ($n = 2$ independent experiments). **f** Confluent SKMel28 cell monolayers were wounded and rhPTX3 were added. Migrated cells in scratch area were photographed and quantified. Bar graphs represent mean ± s.e.m. ($n = 3$ independent experiments performed in duplicate). $^{**}P < 0.01$; $^{***}P < 0.001$ as determined by two-way ANOVA and Bonferroni post-tests

PTX3-depleted cells to transmigrate was rescued by the addition of exogenous PTX3, thereby linking autocrine PTX3 production by melanoma cells to their ability to cross endothelial barriers (Fig. 5e).

Next, we sought to confirm our observations in vivo using a long-term lung colonization assay by bioluminescent melanoma cells [12]. To this end, 1205Lu-Luc + melanoma cells were stably infected with lentiviruses harboring a control shRNA lentivirus (shCtrl) and different shRNAs against PTX3. The efficiency of PTX3 knockdown was assessed by immunoblotting CM from the infected cells (Supplementary Fig. 8a). Further analysis of in vitro cell

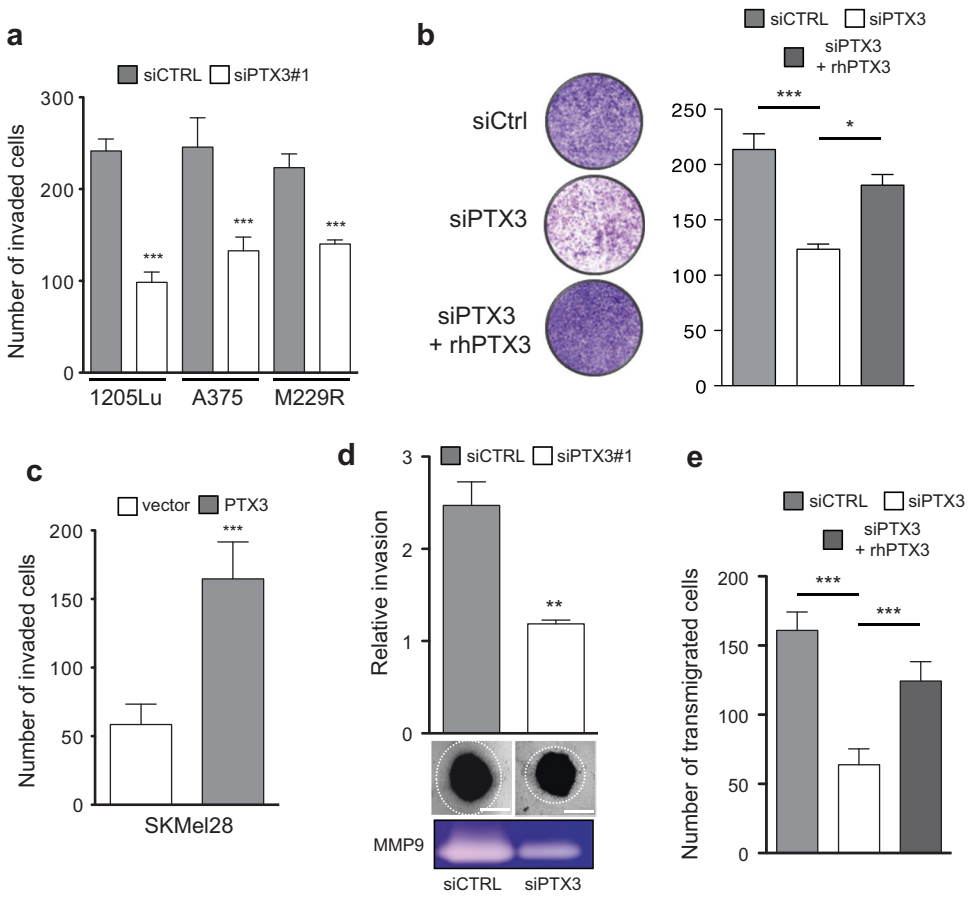

Fig. 5 PTX3 increases melanoma invasiveness in vitro. **a** Transwell invasion assays were performed on siCTRL and siPTX3 transfected cells (1205Lu, A375, M229R) obtained from transfections performed for migration assays (Fig. 4a). Cells were left to migrate for 6 h and counted. Bar graphs show mean number of invaded cells ± s.e.m ($n = 3$ independent experiments). **b** 1205Lu cells were transfected with siCTRL or siPTX3 as described above. After 3 days, serum-stimulated Transwell invasion assays were performed in the presence or not of rhPTX3 (100 ng/ml). Images of one representative insert out of three are shown (left). Bar graphs represent mean ± s.e.m ($n = 2$ independent experiments) (right). **c** Transwell invasion assay was performed as above on SKMel28 cells stably expressing PTX3 or not from Fig. 4b. Cells were left to migrate for 6 h and counted. Bar graphs show mean number ± s.e.m ($n = 3$ independent experiments). **d** Three-dimensional tumor spheroid invasion assay was performed on A375 cells transfected with siCTRL or siPTX3 for 3 days. Tumor cell outgrowth from spheroid edge was visualized by phase contrast microscopy and quantified by ImageJ. Scale bar, 200 µm. Bar graphs show mean ± s.e.m., $n = 2$ independent experiments. Lower panels show collagen zymography on supernatant of A375 cultures. The band of ~110 kDa was identified as MMP-9 by reference to the migration of standard proteins. **e** Transendothelial migration assay was performed on monolayers of primary endothelial cells (HUVECs) grown on Transwell inserts. CMFDA-labeled 1205Lu cells transfected with siCTRL or siPTX3 were then added to the inserts. PTX3 knockdown cells were rescued by adding rhPTX3 (100 ng/ml). Cells were left to migrate for 6 h and cell tracker green-positive cells were counted by fluorescent microscopy. Bar graphs show mean ± s.e.m ($n = 2$ independent experiments). $^{***}P < 0.001$; $^{**}P < 0.01$ as determined by two-way ANOVA

migration in Boyden chamber assays showed that shPTX3 sequence 5 (shPTX3-5) was the most efficient in reducing cell migration compared to shCtrl (Supplementary Fig. 8b). Stable control (shCTRL) and PTX3 (shPTX3-5) knockdown (Fig. 6a) bioluminescent melanoma cells were then injected into the tail vein of nude mice. Bioluminescence imaging (BLI) recorded post injection showed that control and PTX3-depleted cells equally arrested into the lungs after 15 min. However, BLI measurements during the next 15 days revealed a dramatic reduction in lung colonization by PTX3-depleted compared to control cells (Fig. 6b). The quantification of lung colonization by ex vivo BLI at the endpoint of the assay revealed a sixfold reduction in experimental lung metastasis by stable PTX3 knockdown cells compared to control cells (Fig. 6c). Importantly, transient PTX3 knockdown also inhibited melanoma lung extravasation in mice (Supplementary Fig. 9). Finally, using a short-term lung colonization assay [12], we observed that expression of PTX3 in non-metastatic 501Mel cells significantly increased their extravasation into lungs (Fig. 6d).

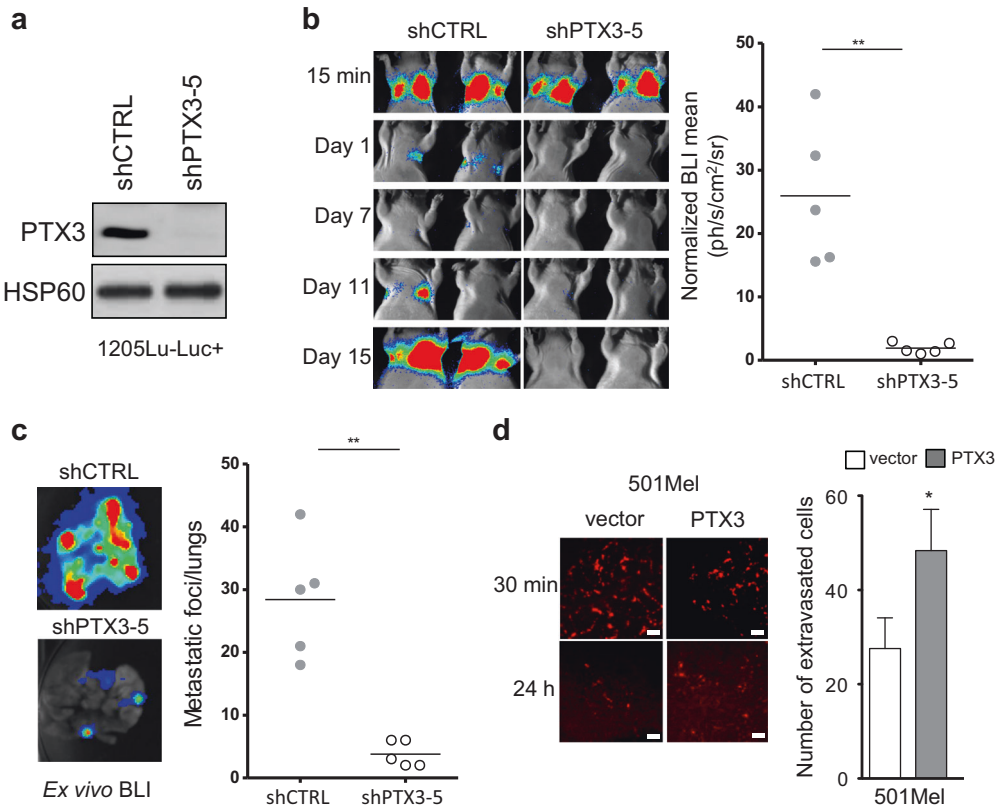

Fig. 6 PTX3 promotes melanoma invasiveness in experimental lung extravasation assay. **a** Immunoblot analysis of PTX3 expression on 1205Lu-Luc + control (shCTRL) and stable PTX3 knockdown (shPTX3-5) cells (see Supplementary Fig. 7 for details). HSP60 was used as a loading control. **b** shCTRL and shPTX3-5 1205Lu-Luc + were injected by tail vein into nude mice ($n = 5$ mice per group) and lung metastasic progression was monitored and quantified using a photon imager. Representative images of photon fluxes produced by bioluminescent melanoma cells from day 0 to day 15 are shown (left panels, $n = 2$) and normalized photon flux (BLI, right graph, $n = 5$) of lungs from control and PTX3-depleted cells. **c** Quantification of lung metastatic foci by ex vivo BLI at the endpoint of the experimental lung extravasation assay performed in **b**. Representative ex vivo BLI imaging of lung mets (left) and quantification of lung metastatic foci per lung (right graph, $n = 5$). **d** Quantification of short-term lung extravasation by 501Mel cells stably expressing PTX3 or not. Cell tracker-labeled melanoma cells that were present within the lungs were counted at the indicated time post injection. Bar graphs show mean ± s.e.m. ($n = 6$ randomly chosen fields) in left panel. Scale bar, 60 µm. $^{**}P < 0.01$, $^{*}P < 0.05$ as determined by unpaired two-tailed Mann–Whitney's test

Altogether, these data suggest that melanoma PTX3 increased the migratory potential of melanoma cells in vivo.

A TLR4-NF-kB-TWIST1 axis is required for melanoma cell migration mediated by PTX3

We next wished to identify the signaling pathways involved in PTX3-mediated melanoma cell migration and invasion. Whereas PTX3 depletion in 1205Lu and M229R cells had no significant effect on the activity of ERK1/2 and AKT (Supplementary Fig. 10), it drastically decreased NF-kB pathway activity, as shown by the reduced level of phosphorylated IKKα/β, IkBα, and NF-kB p65 observed in PTX3-depleted cells (Fig. 7a). Interestingly, reduced NF-kB activity in PTX3-depleted cells decreased the expression of EMT factors TWIST1 and SNAIL. These results suggest that PTX3 activates the NF-kB pathway in melanoma to promote cell migration and invasion through EMT factors. Consistently, IKK targeting in melanoma cells either with IKK inhibitor BMS345541 (Fig. 7b) or with siRNAs directed against IKKα/β (Fig. 7c) reduced EMT factors levels and cell migration. In line with previous reports [10, 11, 20], we confirmed that TWIST1 is an important regulator of melanoma cell migration (Fig. 7d). Conversely, the activation of the NF-kB pathway and TWIST1 expression was significantly increased in 501Mel cells stably expressing PTX3 compared to control cells (Fig. 7e). Using an NF-kB-luciferase reporter construct, we confirmed that overexpression of PTX3 in melanoma cells enhanced NF-kB transcriptional activity in non-stimulated cells and showed additive effects with TNFα stimulation to further increase NF-kB activity (Fig. 7f). Having shown that PTX3 overexpression increased the migration of poorly invasive melanoma cells, we thus examined whether the NF-kB/TWIST pathway participates to this process. A reduction of PTX3-mediated cell migration was observed in PTX3-

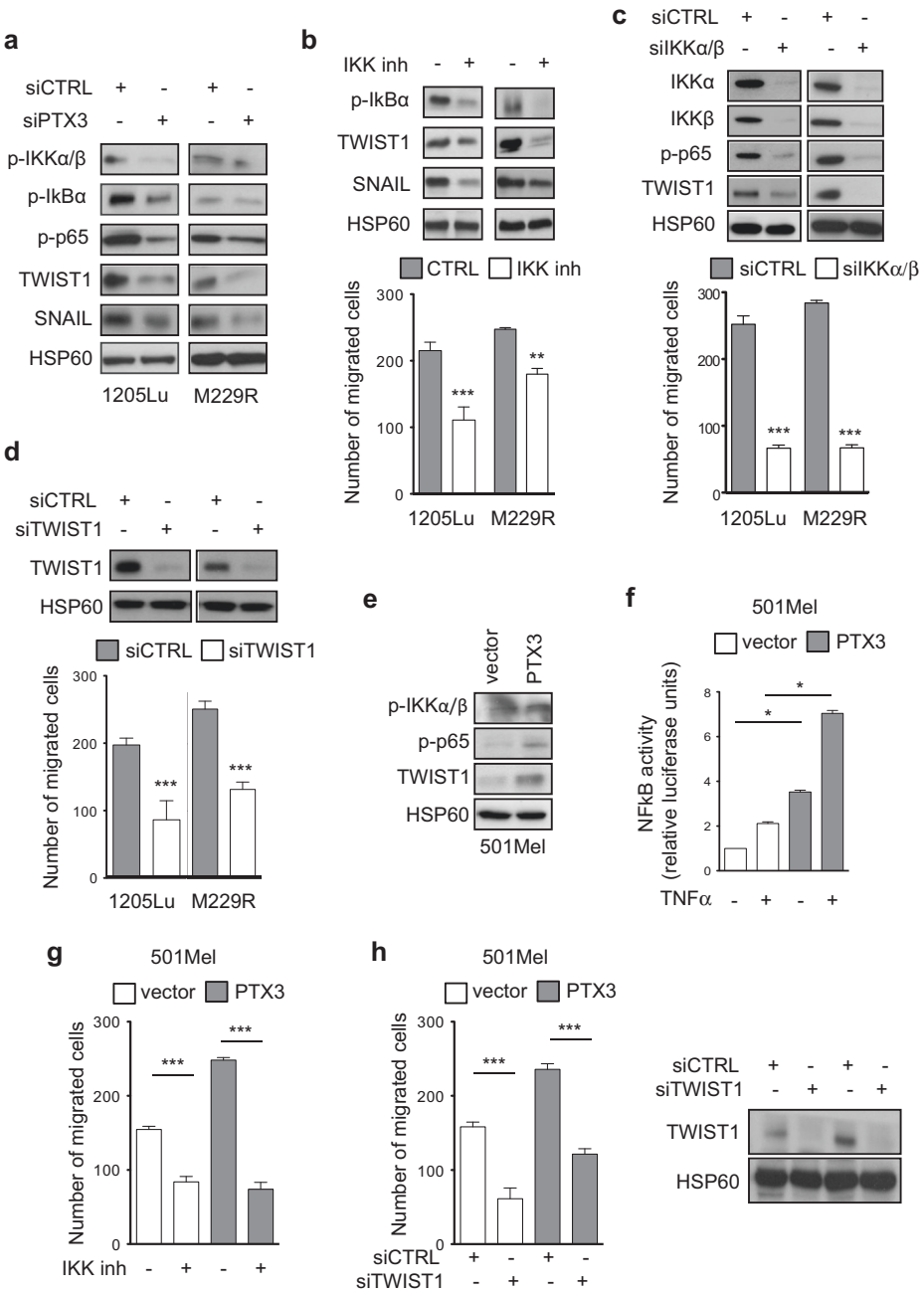

expressing 501Mel cells treated with the IKK inhibitor BMS345541 (Fig. 7g) or transfected with TWIST1 siRNA (Fig. 7h). However, the migration of control cells was also reduced upon IKK inhibition or TWIST1 depletion, indicating that the NF-kB/TWIST axis controls additional PTX3-independent invasive pathways.

Finally, we sought to identify the mechanism through which melanoma-secreted PTX3 endows tumor cells with enhanced migratory potential. Our rescue experiments with exogenous recombinant PTX3 point to the existence of a PTX3 receptor that is expressed at the cell surface of melanoma cells. Previous studies showing that PTX3 mediates antifungal resistance through TLR4/MD-2-mediated signaling [21] and that melanoma cells express functional TLRs including TLR4 [22–24] led us to hypothesize that TLR4 could mediate the effect of PTX3 on melanoma cell migration. The depletion of TLR4 in melanoma cells using two siRNA sequences markedly reduced cell migration (Fig. 8a). Rescue experiments on melanoma cells that were depleted of PTX3 or TLR4 showed that recombinant PTX3 restored the migration of PTX3-silenced cells, whereas recombinant PTX3 was ineffective to restore the

◀ **Fig. 7** PTX3 functions through IKK/NF-kB and TWIST1 to promote melanoma cell migration. **a** 1205Lu and M29R cells were transfected with siCTRL or siPTX3. Cell lysates were immunoblotted with the indicated antibodies. HSP60, loading control. **b** Transwell migration assays were performed on 1205Lu and M229R cells treated with IKK inhibitor BMS345541 (10 μM). Immunoblots with the indicated antibodies are shown. Bar graphs represent mean ± s.e.m ($n = 3$ independent experiments). **c** Transwell migration assays and immunoblot of cell lysate were performed following transfection of 1205Lu and M229R cells with siRNA targeting IKKα and IKKβ (siIKKα/β). Immunoblots for the indicated antibodies are shown. Lower panel represents bar graph of cell migration mean ± s.e.m ($n = 3$ independent experiments). **d** Transwell migration assays were performed on control (siCTRL) or TWIST1-depleted (siTWIST1) 1205Lu and M229R cells. Immunoblots against TWIST1 and HSP60 are shown. Bar graphs show mean ± s.e.m ($n = 3$ independent experiments). **e** Lysates from 501Mel cells stably expressing PTX3 or not were analyzed by immunoblot with the indicated antibodies. **f** 501Mel cells stably expressing PTX3 were transfected with a NF-κB luciferase reporter and stimulated or not with TNF-α (10 nM). Normalized luciferase activity was measured. Bar graphs show mean ± s.e.m ($n = 3$ independent experiments in duplicate). **g** 501Mel cells expressing PTX3 were treated with the IKK inhibitor BMS345541 (10 μM) for 4 h. Transwell migration assays and immunoblot analysis for the indicated antibodies were performed. Bar graphs represent mean ± s.e.m., $n = 3$ experiments. **h** PTX3-expressing 501Mel cells were transfected with siCTRL or siTWIST1. Migration assay was performed as above. Bar graphs show mean ± s.e.m ($n = 2$ independent experiments). $^{***}P < 0.001$, $^{**}P < 0.01$, $^{*}P < 0.05$ as determined by two-way ANOVA and Bonferroni post-tests

migration of TLR4 silenced cells (Fig. 8b). Interestingly, melanoma cells that were depleted of the TLR4 signal transducer MYD88 displayed a reduced motility, decreased NF-kB p65 phosphorylation and TWIST1 expression (Fig. 8c). Consistent with an action of TLR4/MYD88 axis downstream of PTX3, recombinant PTX3 failed to rescue migration of 1205Lu cells that were treated with a MYD88 inhibitory peptide (Supplementary Fig. 11). Finally, we found that the IKK inhibitor BMS345541 impaired the autocrine production of PTX3 by 1205lu cells (Fig. 8d). Together, our results suggest that melanoma-secreted PTX3 could act through a TLR4/MYD88 receptor complex to promote NF-kB activation, TWIST1 and cell migration (Fig. 8e).

Discussion

Upon tumor microenvironment cues, melanoma cells can switch between different cell states characterized by MITF levels and invasive abilities [3–6]. Using a comparative mass spectrometry approach to characterize the melanoma metastatic secretome, we have identified a spectrum of secreted factors and inflammatory mediators that were enriched in conditioned medium of human metastatic cells compared to non-metastatic cells [12]. Here, we further show that PTX3 is one such factor secreted by the $MITF^{low}$ invasive subpopulation of melanomas to promote tumor cell migration through a TLR4/NF-κB signaling pathway. Based on our findings, we propose that PTX3 represents a novel autocrine regulator of melanoma migration and invasiveness.

Analysis of publicly available gene expression databases indicated that high *PTX3* levels correlated with a minority of human melanomas that are associated with a shorter disease-free survival. In addition, our immunohistochemical analysis showed a marked PTX3 immunoreactivity in a fraction of stage IV melanoma but not stage III melanoma tissues, suggesting that high PTX3 expression is associated with melanoma cells from advanced metastatic disease. Accordingly, elevated PTX3 levels were also found increased in blood samples from patients with stage IV metastatic disease. Interestingly, bioinformatic survey of melanoma transcriptional signatures correlated *PTX3* expression to a $MITF^{low}$ invasive subpopulation of melanoma cells. Furthermore, depletion of MITF resulted in increased PTX3 expression in the $MITF^{high}$ proliferative and poorly invasive cell population, suggesting that MITF could negatively regulate *PTX3* expression in melanoma. The $MITF^{low}$ invasive signature has been associated with intrinsic resistance to drugs targeting mutant BRAF and MEK [3, 7, 8]. Consistently, PTX3 expression and secretion was found inversely correlated with MITF expression and positively correlated with mesenchymal markers, such as Fibronectin and PDGFR-β, in cultured melanoma cells that have acquired resistance to the BRAF inhibitor vemurafenib. Importantly, high levels of PTX3 and Fibronectin were also found in a clinical specimen of melanoma that has relapsed from MAPK targeting therapies. Altogether, these observations, which link PTX3 expression to a subpopulation of dedifferentiated and invasive $MITF^{low}$ melanoma cells, underscore the notion that PTX3 may represent a novel potential indicator of advanced metastatic and/or drug-refractory melanoma.

The acquisition of migratory and invasive abilities by melanoma cells involves induction of mesenchymal traits by transcription factors, including those of the SNAIL, TWIST, and ZEB families [6, 9–11]. Accordingly, autocrine production of PTX3 by invasive melanoma cells was found to induce an IKK/NFκB signaling pathway that activated the pro-invasive matrix metalloproteinase MMP-9 and the expression of the EMT-inducing factor TWIST1, leading to tumor cell migration and invasion. Thus, we identified PTX3 as a novel crucial regulator of melanoma cell invasive behavior. These observations appear to be in striking contrast with a previous study in which PTX3 was described as an intrinsic oncosuppressive protein in certain melanoma cells [25]. However, there are consistent with other studies that have attributed to PTX3 a cancer-supportive activity. For example, knocking down PTX3 in

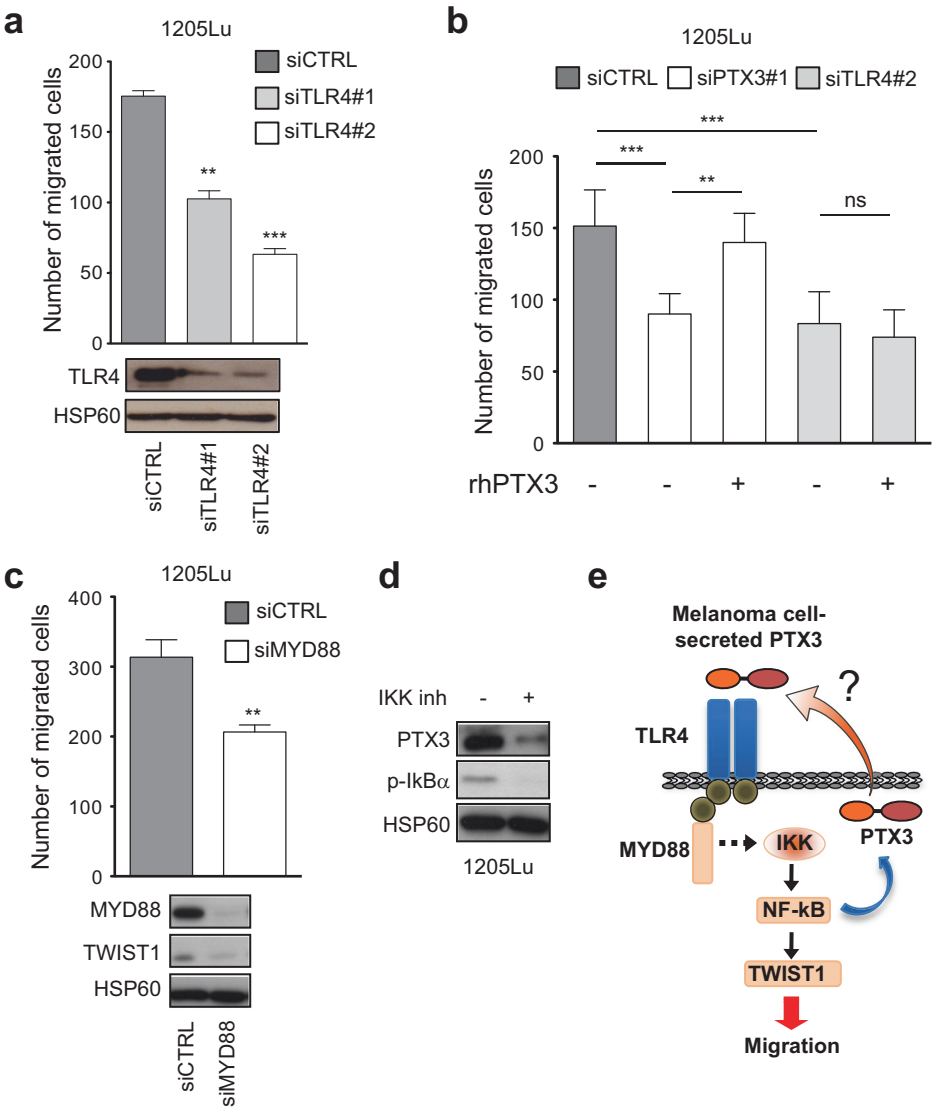

Fig. 8 TLR4/MYD88 expression is required for PTX3-induced melanoma cell migration. **a** Transwell migration assays were performed on 1205Lu cells transfected with siCTRL or two different siTLR4. Immunoblot analysis shows TLR4 depletion. HSP60, loading control. Bar graphs represent mean of migrated cells ± s.e.m ($n = 3$ independent experiments). **b** 1205Lu cells were transfected with siPTX3 or siTLR4. After 3 days, cells were stimulated or not with rhPTX3 for 4 h and Transwell migration assays were performed. Bar graphs show migration mean ± s.e.m ($n = 2$ independent experiments). **c** Transwell migration assays on control and MYD88-depleted 1205Lu cells. Bar graphs show migration mean ± s.e.m ($n = 2$ independent experiments). MYD88 and TWIST1 levels were controlled by immunoblot. **d** 1205Lu cells were treated with the IKK inhibitor BMS345541 and PTX3 expression was assessed by immunoblot. **e** Schematic model of PTX3 autocrine action on melanoma cell migration. $^{***}P < 0.001$, $^{**}P < 0.01$ as determined by two-way ANOVA and Bonferroni post-tests

cervical cancer cells decreases migratory and invasive abilities in vitro and metastatic potential by inhibiting MMP-2/9 and the urokinase plasminogen activator (uPA) [26]. In head and neck squamous cell carcinoma (HNSCC), autocrine production of EGF-induced PTX3 expression promotes cell migration, invasion, and lung metastasis through the upregulation of Fibronectin, MMP-9 and Vimentin [27, 28]. Remarkably, our results indicate that overexpression of PTX3 autonomously instigated a migratory and invasive phenotype to poorly invasive $MITF^{high}$ melanoma cells. The observation that recombinant or melanoma-derived PTX3 increased the migration of poorly motile melanoma cell lines further suggests that PTX3 acts both as a paracrine and autocrine factor in the heterogeneous melanoma cell population.

Additionally, we have addressed how PTX3 modulates melanoma cell biological properties. A study showing that PTX3 mediates antifungal resistance through TLR4/MD-2-mediated signaling [21] suggested that PTX3 could exogenously promote melanoma migration through a TLR4 signaling axis. Previous reports showing that melanocytes and melanoma cells express functional TLRs including TLR4 [22–24], and that TLR4 promotes the migration of melanoma cells independently of its canonical agonist LPS [24] further reinforced this hypothesis. Consistently, we found that TLR4 and MYD88 knockdown or targeting significantly inhibited PTX3-induced melanoma cell migration and TWIST1 expression. However, whether melanoma-derived PTX3 directly associates with TLR4 on the surface of melanoma cells remains to be shown. In addition, the exact mechanism by which PTX3 regulates NF-kB-dependent expression of the EMT factor TWIST1 has yet to be determined. It is possible that PTX3 triggers NF-kB-mediated transcriptional upregulation of TWIST1,

in similar ways to what was described for TNFα-induced TWIST1 expression in breast cancer cells [29]. Interestingly, TLR4 expression has been associated with a shorter relapse-free survival in cutaneous malignant melanoma [23], suggesting that a feed-forward PTX3/TLR4/NF-kB signaling pathway favors melanoma invasive phenotype. In support of this notion is the finding that IKKα/β activity was necessary to the autocrine production of PTX3 by invasive melanoma cells.

PTX3 plays a major non-redundant role in the humoral innate immunity during complement activation and pathogen recognition, inflammatory responses, and tissue repair [13, 14]. In contrast, its function in tumor development and metastasis remains largely debated in line with studies reporting either its oncosuppressive [15, 30] or its protumorigenic activity [27, 31–33] (recently reviewed in ref. [34]. The emerging model for PTX3 implication in tumorigenesis points to an extrinsic activity as an oncosuppressive factor in cancer-related inflammation. The production of PTX3 by tumor microenvironment-associated macrophages (TAMs) and endothelial cells was shown to impede the tumor-promoting inflammation that is driven by complement activation [15]. In addition, PTX3 overexpression or targeting prevented FGF-dependent tumor angiogenesis and growth in a variety of cancer models such as prostate cancers [35, 36], steroid hormone-regulated tumors [37], and breast cancers [38]. Similarly, in melanoma, PTX3 has been shown to hamper FGF-driven cell invasiveness and metastatic potential [25]. On the contrary, our study supports a role of PTX3 as an intrinsic prometastatic protein regulating cell motility in a subpopulation of $MITF^{low}$ invasive melanoma. Our data are consistent with studies supporting the role of PTX3 as an intrinsic oncogenic protein in lung [39], head and neck [27], cervical [26], and gastric [31] cancers. Similar to our findings, studies have also correlated high levels of tissues and/or circulating PTX3 in patients with lung [40], breast [38], ovarian [41], pancreatic [42], liver [43], glioma [44], and prostate [45] tumors. In addition, PTX3 represents an effector of oncogenic PI3K signaling that maintains stem cell-like traits in basal-like breast cancers [33]. Collectively, these observations suggest that PTX3 represents a pleiotropic cancer biomarker and a cell context-dependent therapeutic target.

Chronic inflammation is implicated in tumorigenesis and metastasis through the recruitment and activation of TAMs that produce inflammatory cytokines, such as TNFα, which in turn activate the NF-kB pathway [46, 47]. In melanoma, TNFα was shown to promote NF-kB-dependent BRAF inhibitor resistance [48] and to suppress MITF expression, thereby initiating an inflammation-induced dedifferentiation program [49]. Of note, $MITF^{low}$ invasive melanoma cells were also found to secrete high amounts of other inflammatory factors, such as IL-6 (Supplementary Fig. 1 and Supplementary Table 1), which has been involved in TWIST-dependent cell invasiveness [20], and our in silico analysis associated high *PTX3* expression in melanoma with a hallmark inflammatory response gene signature. Our experiments further indicate that targeting PTX3-induced IKK/NF-kB pathway is effective to reduce melanoma cell migration. This adds to the list of signaling pathways that contribute to the regulation of the invasive abilities of melanoma cells. Altogether, our data support a model in which a subpopulation of metastatic melanomas have acquired an autoinflammatory-like phenotype characterized by an autoamplifying PTX3/TLR4/NF-kB invasive signaling pathway.

In summary, our study supports a key role of tumor-derived PTX3 for melanoma migration and provides a rationale for targeting PTX3-mediated NF-kB invasive signaling as part of a novel therapeutic approach to treat the metastatic disease.

Materials and methods

Cells, reagents, and plasmids

A375, 1205Lu, MeWo, WM35, WM793, and SKMel28 melanoma cell lines were from ATCC. 1205Lu cells that were engineered to express a luciferase reporter (1205Lu-Luc + cells) were described before [12]. Other melanoma cell lines and patient melanoma cells were obtained as described before [50]. All cell lines were tested and found to be mycoplasma-negative. Melanoma cells were cultured in Dulbecco's modified Eagle Medium (DMEM) plus 7% Fetal Bovine Serum (FBS) (Thermo Fisher Scientific). Conditioned media (CM) from melanoma cells were prepared as previously described [12].

Human umbilical vascular endothelial cells (HUVECs) were cultured in complete EGM2 Bullet Kit medium supplemented with 2% FBS and full supplements (Lonza). All other culture reagents and Cell Tracker dyes were from Thermo Fischer Scientific. The source for other reagents was as follows: recombinant human PTX3 (Bio-Techne), MYD88 Inhibitor peptide (NOVUS Biologicals), IKK inhibitor BMS345541 (Selleckchem), chemicals (Sigma-Aldrich). The PTX3 complementary DNA was amplified by PCR from 1205Lu cells using the primers: Fwd: ACTCG AGCCACCATGCATCTCCTTGCGATTCTG; Rev: TAG GATCCTTATGAAACATACTGAGCTCCT and subcloned in the pIRES2-EGFP vector (Takara) using *BamHI/XhoI* restriction sites to generate the pPTX3-IRES-EGFP vector. The PTX3-IRES-EGFP cassette was subsequently subcloned into the pLPCX retroviral vector using *XhoI/NotI* restriction sites to generate the pLPCX-PTX3-pIRES2-EGFP vector. 501Mel-CTRL and 501Mel-PTX3 cells were

obtained following pIRES2-EGFP and pPTX3-IRES-EGFP transfection, respectively and geneticin selection. SKMel28-CTRL and SKMel28-PTX3 were generated by retroviral transduction with pLPCX and pLPCX-PTX3-IRES2-EGFP, respectively, and puromycin selection. The NF-κB luciferase reporter vector was from BPS Bioscience.

RNAi studies

Negative control and PTX3 siRNA duplexes were designed by Thermo Fisher Scientific. MITF (sc-35934), MYD88 (sc-35986), and TWIST1 (sc-38604) siRNAs were from Santa Cruz Biotechnology. IKKα, IKKβ, and TLR4 siRNAs were from Dharmacon (CO, USA). Transfection of siRNA was carried out using Lipofectamine RNAiMAX (Thermo Fisher Scientific) at a final concentration of 25 or 50 nM. Unless stated otherwise, cells were assayed 3 days post transfection. Lentiviral vectors for stable knockdown of PTX3 (NM_002852) in melanoma cells were TRC1.5-pLKO.1-puro vectors (shPTX3-1 to 5) (Genomic center, University of Minnesota, USA). Lentiviral, packaging (psPAX2) and enveloppe (pMD2.0 G) vectors were transfected into HEK293T cells and virus-containing supernatant fractions were harvested after 72 h. The supernatant fractions were filtered and used to infect bioluminescent 1205Lu cells (1205Lu-Luc +) that were described before [12]. Transduced cells were selected with 2 µg/ml puromycin for 3 weeks. The efficiency of PTX3 knockdown was assessed by immunoblotting and analysis of in vitro cell migration using modified Boyden chambers. The PTX3 knockdown cells that were selected for in vivo studies were transduced by lentivirus harboring the shPTX3-5 sequence (TRCN0000149744, 5′-CCGGGAGG AGCTCAGTATGTTTCATCTCGAGATGAAACATACT-GAGCTCCTCTTTTTTG-3′).

Immunohistochemistry and immunoblot analysis

Immunohistochemistry and immunoblot analysis were performed as described before [12]. IHC analysis was performed on melanoma tissue microarrays (US Biomax) using PTX3 antibody (HPA069320, Sigma-Aldrich; 1:50). For immunoblotting, the following antibodies were used at 1:1000: SPARC (Bio-Techne), PTX3 (Enzo Life Sciences, Switzerland), HSP90, HSP60, TLR4, Fibronectin, ERK2 (Santa Cruz Biotechnology), MITF (Thermo Fisher Scientific), TWIST1 (Abcam, UK), SNAIL, phospho-IKKα/β (Ser176/180), NF-kB p65, phospho-NF-kB p65 (Ser536), IκBα (L35A5), phosphor-IκBα (Ser32/36), IKKα, IKKβ, MYD88, phospho-AKT (Ser473), phospho-ERK1/2 (Thr202/Tyr204), phospho-PRAS40 (Thr246), phospho-c-Jun (Ser63) (Cell Signaling Technology).

Migration, invasion, and in vitro scratch assays

Serum-stimulated chemotaxis, invasion, and transendothelial migration were monitored using modified Boyden chambers (8 µm pores, Sigma) as described before [12]. For invasion assays, the upper side of the filter was coated with 0.5 mg/ml matrigel (Corning, NY, USA). Migrated cells were stained with crystal violet and counted (four fields randomly per well). For transendothelial migration, 10^5 HUVECs were grown in the upper chamber of gelatin-coated Transwell inserts and treated with human TNFα (10 ng/ml) for 16 h. Melanoma cells were allowed to migrate for 6 h and migrated cells were visualized and quantified as before [12]. Pictures of five random fields were captured for quantification using NIH ImageJ analysis software. For scratch assays, melanoma cells were grown ~80% confluence in 6-well plates. Wounds were generated using a sterile 200 µl pipette tip across each well. Following treatment with rhPTX3 or CM, pictures of four random fields were captured using an imaging station and the number of migrated cells in wounded area was counted with NIH ImageJ analysis software.

Spheroid invasion assay and zymography

Melanoma three-dimensional (3D) spheroids were generated as described [51]. Pictures of migrating cells were taken at day 0 and day 3. Relative invasion was determined using the ImageJ software as the ratio between migration area at day 3 and migration area at day 0. CM from melanoma cells were analyzed by collagen zymography as previously described [52].

Promoter reporter assay

Melanoma cells were transfected with NF-κB-luciferase and β-Galactosidase reporter plasmids. Forty-eight hours after transfection, cells were lysed and luciferase and β-galactosidase activities were measured as described before [53]. Relative NF-κB promoter activity was calculated following normalization against β-galactosidase activity.

In vivo experiments and immunostaining

All mouse experiments were carried out in accordance with the Institutional Animal Care and local ethics committees. For experimental lung metastasis studies, 5-week-old female nude mice (Harlan) were intravenously injected with 1205Lu-Luc+ cells (1×10^6) that were transduced with a non-targeting shRNA lentivirus (shCTRL) or a PTX3-targeting shRNA lentivirus (shPTX3-5). Images were acquired using a Photon Imager (Biospace Lab) on mice

injected i.p. with 50 mg/kg D-luciferin (PerkinElmer). Lung metastasis was monitored and quantified using BLI [12]. In a second set of experiments, short-term lung colonization assays were performed with Cell Tracker Orange-stained 501Mel cells stably expressing PTX3 or not. Cells were intravenously injected in 5-week-old female nude mice that were sacrificed either 30 min or 24 h later. Lungs were perfused with PBS, fixed in 4% paraformaldehyde, OCT-embedded, cryosectioned, immunostained and imaged using a confocal microscope as described [12].

ELISA assay

The levels of PTX3 in CM of melanoma cell lines or in human serum samples were measured using the human PTX3 Quantikine ELISA kit (Bio-Techne) as per the manufacturer's protocol. Serum samples were obtained from consenting metastatic melanoma patients through the Dermatology Department of Nice University Hospital (Nice, France) or from healthy volunteers as controls. Results are from two independent experiments performed in triplicate.

Analysis of gene expression from human databases

Publicly available gene expression data sets of human melanoma samples were used to analyze *PTX3* levels in melanoma progression (GSE3189). From GEO database, we also examined the Mannheim (GSE4843), Philadelphia (GSE4841), and Zurich (GSE4840) cohorts. Proliferative and invasive melanoma subgroups were defined according to literature mined gene signatures [4]. Gene expression of *PTX3* was also examined in data sets derived from patient tumor biopsies before and after development of drug resistance to Vemurafenib (GEO accession number GSE50535) [54]. Normalized data were analyzed using GraphPad Prism (GraphPad software, CA, USA). Survival data from the skin melanoma TCGA database were retrieved using cBioPortal (cbioportal.org). Gene set enrichment analysis (GSEA) was performed as described before [55].

Statistical analysis

Unless otherwise stated, all the experiments were repeated at least three times and representative data/images are shown. Statistical data analysis was performed using GraphPad Prism software. Unpaired two-tailed Mann–Whitney tests or two-way ANOVA tests with Bonferroni post-tests were used for statistical comparisons. Error bars are mean ± s.e.m.

Acknowledgements We thank RS Lo and R Ballotti for melanoma cells. We acknowledge the C3M animal and imaging (Microscopy and Imaging platform Côte d'Azur, MICA) facilities. This work was supported by Ligue Contre le Cancer, Fondation ARC, Fondation de France and the French Government (National Research Agency, ANR) through the "Investments for the Future" LABEX SIGNALIFE: program reference # ANR-11-LABX-0028-01. We also thank financial supports by Conseil Général des Alpes-Maritimes, Canceropôle PACA and Région PACA. MR was a recipient of a post-doctoral fellowship from Fondation ARC. The Marseille Proteomic facility (MaP; http://map.univmed.fr/) is supported by IBiSA (Infrastructures Biologie Santé et Agronomie), Canceropôle PACA, Région PACA, and Institut Paoli-Calmettes.

Author contributions MD, STD, and MR designed the study. MD and STD wrote the manuscript. MR, CG, MT and RBJ performed the experiments and analyzed the data with the help of EG, FL, and VP. MG provided technical expertize in microscopy. SA performed mass spectrometry analyses. J-PL and HM contributed clinical samples and expertize.

Compliance with ethical standards

Conflict of interest The authors declare that they have no conflict of interest.

Publisher's note: Springer Nature remains neutral with regard to jurisdictional claims in published maps and institutional affiliations.

References

1. Flaherty KT, Hodi FS, Fisher DE. From genes to drugs: targeted strategies for melanoma. Nat Rev Cancer. 2012;12:349–61.
2. Holderfield M, Deuker MM, McCormick F, McMahon M. Targeting RAF kinases for cancer therapy: BRAF-mutated melanoma and beyond. Nat Rev Cancer. 2014;14:455–67.
3. Kemper K, de Goeje PL, Peeper DS, van Amerongen R. Phenotype switching: tumor cell plasticity as a resistance mechanism and target for therapy. Cancer Res. 2014;74:5937–41.
4. Widmer DS, Cheng PF, Eichhoff OM, Belloni BC, Zipser MC, Schlegel NC, et al. Systematic classification of melanoma cells by phenotype-specific gene expression mapping. Pigment Cell Melanoma Res. 2012;25:343–53.
5. Cheli Y, Giuliano S, Fenouille N, Allegra M, Hofman V, Hofman P, et al. Hypoxia and MITF control metastatic behaviour in mouse and human melanoma cells. Oncogene. 2012;31:2461–70.
6. Verfaillie A, Imrichova H, Atak ZK, Dewaele M, Rambow F, Hulselmans G, et al. Decoding the regulatory landscape of melanoma reveals TEADS as regulators of the invasive cell state. Nat Commun. 2015;6:6683.
7. Muller J, Krijgsman O, Tsoi J, Robert L, Hugo W, Song C, et al. Low MITF/AXL ratio predicts early resistance to multiple targeted drugs in melanoma. Nat Commun. 2014;5:5712.
8. Shaffer SM, Dunagin MC, Torborg SR, Torre EA, Emert B, Krepler C, et al. Rare cell variability and drug-induced reprogramming as a mode of cancer drug resistance. Nature. 2017;546:431–5.
9. Fenouille N, Tichet M, Dufies M, Pottier A, Mogha A, Soo JK, et al. The epithelial-mesenchymal transition (EMT) regulatory factor SLUG (SNAI2) is a downstream target of SPARC and AKT in promoting melanoma cell invasion. PLoS ONE. 2012;7:e40378.
10. Weiss MB, Abel EV, Mayberry MM, Basile KJ, Berger AC, Aplin AE. TWIST1 is an ERK1/2 effector that promotes invasion and regulates MMP-1 expression in human melanoma cells. Cancer Res. 2012;72:6382–92.

11. Caramel J, Papadogeorgakis E, Hill L, Browne GJ, Richard G, Wierinckx A, et al. A switch in the expression of embryonic EMT-inducers drives the development of malignant melanoma. Cancer cell 2013;24:466–80.
12. Tichet M, Prod'Homme V, Fenouille N, Ambrosetti D, Mallavialle A, Cerezo M, et al. Tumour-derived SPARC drives vascular permeability and extravasation through endothelial VCAM1 signalling to promote metastasis. Nat Commun. 2015;6:6993.
13. Garlanda C, Jaillon S, Doni A, Bottazzi B, Mantovani APTX3. a humoral pattern recognition molecule at the interface between microbe and matrix recognition. Curr Opin Immunol. 2016;38:39–44.
14. Bottazzi B, Inforzato A, Messa M, Barbagallo M, Magrini E, Garlanda C, et al. The pentraxins PTX3 and SAP in innate immunity, regulation of inflammation and tissue remodelling. J Hepatol. 2016;64:1416–27.
15. Bonavita E, Gentile S, Rubino M, Maina V, Papait R, Kunderfranco P, et al. PTX3 is an extrinsic oncosuppressor regulating complement-dependent inflammation in cancer. Cell. 2015;160:700–14.
16. Magrini E, Mantovani A, Garlanda C. The dual complexity of PTX3 in health and disease: a balancing act? Trends Mol Med. 2016;22:497–510.
17. Nazarian R, Shi H, Wang Q, Kong X, Koya RC, Lee H, et al. Melanomas acquire resistance to B-RAF(V600E) inhibition by RTK or N-RAS upregulation. Nature. 2010;468:973–7.
18. Titz B, Lomova A, Le A, Hugo W, Kong X, Ten Hoeve J, et al. JUN dependency in distinct early and late BRAF inhibition adaptation states of melanoma. Cell Discov. 2016;2:16028.
19. Obenauf AC, Massague J. Surviving at a distance: organ-specific metastasis. Trends Cancer. 2015;1:76–91.
20. Na YR, Lee JS, Lee SJ, Seok SH. Interleukin-6-induced Twist andx N-cadherin enhance melanoma cell metastasis. Melanoma Res. 2013;23:434–43.
21. Bozza S, Campo S, Arseni B, Inforzato A, Ragnar L, Bottazzi B, et al. PTX3 binds MD-2 and promotes TRIF-dependent immune protection in aspergillosis. J Immunol. 2014;193:2340–8.
22. Ahn JH, Park TJ, Jin SH, Kang HY. Human melanocytes express functional Toll-like receptor 4. Exp Dermatol. 2008;17:412–7.
23. Eiro N, Ovies C, Fernandez-Garcia B, Alvarez-Cuesta CC, Gonzalez L, Gonzalez LO, et al. Expression of TLR3, 4, 7 and 9 in cutaneous malignant melanoma: relationship with clinicopathological characteristics and prognosis. Arch Dermatol Res. 2013;305:59–67.
24. Takazawa Y, Kiniwa Y, Ogawa E, Uchiyama A, Ashida A, Uhara H, et al. Toll-like receptor 4 signaling promotes the migration of human melanoma cells. Tohoku J Exp Med. 2014;234:57–65.
25. Ronca R, Di Salle E, Giacomini A, Leali D, Alessi P, Coltrini D, et al. Long pentraxin-3 inhibits epithelial-mesenchymal transition in melanoma cells. Mol Cancer Ther. 2013;12:2760–71.
26. Ying TH, Lee CH, Chiou HL, Yang SF, Lin CL, Hung CH, et al. Knockdown of Pentraxin 3 suppresses tumorigenicity and metastasis of human cervical cancer cells. Sci Rep. 2016;6:29385.
27. Chang WC, Wu SL, Huang WC, Hsu JY, Chan SH, Wang JM, et al. PTX3 gene activation in EGF-induced head and neck cancer cell metastasis. Oncotarget. 2015;6:7741–57.
28. Chan SH, Tsai JP, Shen CJ, Liao YH, Chen BK. Oleate-induced PTX3 promotes head and neck squamous cell carcinoma metastasis through the up-regulation of vimentin. Oncotarget. 2017;8:41364–78.
29. Li CW, Xia W, Huo L, Lim SO, Wu Y, Hsu JL, et al. Epithelial-mesenchymal transition induced by TNF-alpha requires NF-kappaB-mediated transcriptional upregulation of Twist1. Cancer Res. 2012;72:1290–300.
30. Rubino M, Kunderfranco P, Basso G, Greco CM, Pasqualini F, Serio S, et al. Epigenetic regulation of the extrinsic oncosuppressor PTX3 gene in inflammation and cancer. Oncoimmunology. 2017;6:e1333215.
31. Choi B, Lee EJ, Park YS, Kim SM, Kim EY, Song Y, et al. Pentraxin-3 silencing suppresses gastric cancer-related inflammation by inhibiting chemotactic migration of macrophages. Anticancer Res. 2015;35:2663–8.
32. Tung JN, Ko CP, Yang SF, Cheng CW, Chen PN, Chang CY, et al. Inhibition of pentraxin 3 in glioma cells impairs proliferation and invasion in vitro and in vivo. J Neurooncol. 2016;129:201–9.
33. Thomas C, Henry W, Cuiffo BG, Collmann AY, Marangoni E, Benhamo V, et al. Pentraxin-3 is a PI3K signaling target that promotes stem cell-like traits in basal-like breast cancers. Sci Signal. 2017;10:eaah4674.
34. Giacomini A, Ghedini GC, Presta M, Ronca R. Long pentraxin 3: a novel multifaceted player in cancer. Biochim Biophys Acta, Rev Cancer. 2018;1869:53–63.
35. Ronca R, Alessi P, Coltrini D, Di Salle E, Giacomini A, Leali D, et al. Long pentraxin-3 as an epithelial-stromal fibroblast growth factor-targeting inhibitor in prostate cancer. J Pathol. 2013;230:228–38.
36. Ronca R, Giacomini A, Di Salle E, Coltrini D, Pagano K, Ragona L, et al. Long-pentraxin 3 derivative as a small-molecule fgf trap for cancer therapy. Cancer Cell. 2015;28:225–39.
37. Leali D, Alessi P, Coltrini D, Ronca R, Corsini M, Nardo G, et al. Long pentraxin-3 inhibits FGF8b-dependent angiogenesis and growth of steroid hormone-regulated tumors. Mol Cancer Ther. 2011;10:1600–10.
38. Margheri F, Serrati S, Lapucci A, Anastasia C, Giusti B, Pucci M, et al. Systemic sclerosis-endothelial cell antiangiogenic pentraxin 3 and matrix metalloprotease 12 control human breast cancer tumor vascularization and development in mice. Neoplasia. 2009;11:1106–15.
39. Hu FQ, Qiao T, Xie X, Hu R, Xiao HB. Knockdown of the inflammatory factor pentraxin-3 suppresses growth and invasion of lung adenocarcinoma through the AKT and NF-kappa B pathways. J Biol Regul Homeost Agents. 2014;28:649–57.
40. Diamandis EP, Goodglick L, Planque C, Thornquist MD. Pentraxin-3 is a novel biomarker of lung carcinoma. Clin Cancer Res: Off J Am Assoc Cancer Res. 2011;17:2395–9.
41. Tothill RW, Tinker AV, George J, Brown R, Fox SB, Lade S, et al. Novel molecular subtypes of serous and endometrioid ovarian cancer linked to clinical outcome. Clin Cancer Res: Off J Am Assoc Cancer Res. 2008;14:5198–208.
42. Kondo S, Ueno H, Hosoi H, Hashimoto J, Morizane C, Koizumi F, et al. Clinical impact of pentraxin family expression on prognosis of pancreatic carcinoma. Br J Cancer. 2013;109:739–46.
43. Carmo RF, Aroucha D, Vasconcelos LR, Pereira LM, Moura P, Cavalcanti MS. Genetic variation in PTX3 and plasma levels associated with hepatocellular carcinoma in patients with HCV. J Viral Hepat. 2016;23:116–22.
44. Locatelli M, Ferrero S, Martinelli Boneschi F, Boiocchi L, Zavanone M, Maria Gaini S, et al. The long pentraxin PTX3 as a correlate of cancer-related inflammation and prognosis of malignancy in gliomas. J Neuroimmunol. 2013;260:99–106.
45. Ravenna L, Sale P, Di Vito M, Russo A, Salvatori L, Tafani M, et al. Up-regulation of the inflammatory-reparative phenotype in human prostate carcinoma. Prostate. 2009;69:1245–55.
46. Coussens LM, Werb Z. Inflammation and cancer. Nature. 2002;420:860–7.
47. Karin M, Greten FR. NF-kappaB: linking inflammation and immunity to cancer development and progression. Nat Rev Immunol. 2005;5:749–59.
48. Shao Y, Le K, Cheng H, Aplin AE. NF-kappaB regulation of c-FLIP promotes TNFalpha-mediated RAF inhibitor resistance in melanoma. J Invest Dermatol. 2015;135:1839–48.
49. Riesenberg S, Groetchen A, Siddaway R, Bald T, Reinhardt J, Smorra D, et al. MITF and c-Jun antagonism interconnects

melanoma dedifferentiation with pro-inflammatory cytokine responsiveness and myeloid cell recruitment. Nat Commun. 2015;6:8755.
50. Didier R, Mallavialle A, Ben Jouira R, Domdom MA, Tichet M, Auberger P, et al. Targeting the proteasome-associated deubiquitinating enzyme USP14 impairs melanoma cell survival and overcomes resistance to MAPK-targeting therapies. Mol Cancer Ther. 2018;17:1416–29.
51. Bailet O, Fenouille N, Abbe P, Robert G, Rocchi S, Gonthier N, et al. Spleen tyrosine kinase functions as a tumor suppressor in melanoma cells by inducing senescence-like growth arrest. Cancer Res. 2009;69:2748–56.
52. Robert G, Gaggioli C, Bailet O, Chavey C, Abbe P, Aberdam E, et al. SPARC represses E-cadherin and induces mesenchymal transition during melanoma development. Cancer Res. 2006;66:7516–23.
53. Fenouille N, Robert G, Tichet M, Puissant A, Dufies M, Rocchi S, et al. Thep53/p21(Cip1/ Waf1) pathway mediates the effects of SPARC on melanoma cell cycle progression. Pigment Cell Melanoma Res. 2011;24:219–32.
54. Sun C, Wang L, Huang S, Heynen GJ, Prahallad A, Robert C, et al. Reversible and adaptive resistance to BRAF(V600E) inhibition in melanoma. Nature. 2014;508:118–22.
55. Ohanna M, Cerezo M, Nottet N, Bille K, Didier R, Beranger G, et al. Pivotal role of NAMPT in the switch of melanoma cells toward an invasive and drug-resistant phenotype. Genes Dev. 2018;32:448–61.